



NEW APPROACH ON THE ROLE OF A POLYMER MATRIX IN THE STRONG TEXTURATION OF ZnO NANOPOWDERS

Ioana Raluca PREPELITA,^a Narcisa VRINCEANU,^{b,c,*} Roxana CHIRITA^a, Romeo Petru DOBRIN^a,
Ovidiu Eugen ALEXINSCHI,^a Florin BRINZA,^d Bogdan Alexandru HAGIU^e and Mirela Petruta SUCHEA^{b,f}

^a“Gr.T. Popa” University of Medicine and Pharmacy of Iași, Faculty of Medicine, Department of Psychiatry,
16 Universitatii Street, 700115, Iasi, Roumania

^b“Al. I. Cuza” University of Iași, Faculty of Chemistry, 11 Carol I Street, 700506, Roumania

^c“Lucian Blaga” University of Sibiu, Faculty of Engineering, Department of Industrial Machines and Equipments,
10, Victoriei Boulevard, 550024, Sibiu, Roumania

^d“Al. I. Cuza” University of Iași, Faculty of Physics, 11 Carol I Street, 700506, Roumania

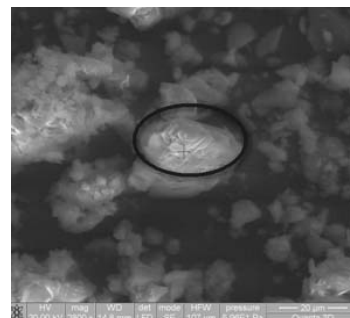
^e“Al. I. Cuza” University of Iași, Faculty of Physical Education and Sports, 3, Toma Cozma Street, 700554, Roumania

^fCenter of Materials Technology and Laser, School of Applied Technology,
Electrical Engineering Department, Technological Educational Institute of Crete, Estavromenos, 71004, Heraklion, Greece

Received June 18, 2013

The present study investigates the efficiency of a new synthesis sol-gel method providing both architectural structure and stabilization of strong textures consisting of ZnO nanoparticles dispersions, using a polymer matrix, meaning a cyclic oligosaccharide, β -cyclodextrin (*i.e.* MCT - MonoChloroTriazinyl- β -cyclodextrin). ZnO has been synthesized by reacting of zinc nitrate with sodium hydroxide in the presence of MCT by a facile wet-chemical method. Synthesized powder was investigated using X-ray diffraction technique and scanning electron microscopy. X-Ray diffractogram revealed some crystalline plans of ZnO - MCT complex structure. SEM images show a lamellar structure similar to biogenic calcites in the presence of echinoderm intracrystalline proteins. Presence of MCT during ZnO nucleation can ensure formation of micro-pellets with nanometric thickness. This texture is in according with the morphology of the single crystal elements, suggesting that MCT may also have influence in the shape of the crystal during its growth.

The study demonstrates the fundamental role playing by polymer involving in the patterning of ZnO composites. The lamellar morphology of obtained samples proved the biomimetic assembled aspect of the present study.



INTRODUCTION

There is an abundant research concerning various methods to obtain well-defined ZnO nanomaterials preparation, such aqueous precipitate synthesis,¹ vapor transport,² chemical vapor deposition (CVD),³ hydrothermal process assisted by microemulsion-mediated and sol-gel derived process.^{4,5} One of the versatile ways to obtain ZnO nanomaterials is thermal decomposition of zinc salt, choosing zinc acetate ($\text{Zn}(\text{CH}_3\text{COO})_2$) as the precursor due to its high solubility and low

decomposition temperature.⁶ All these above mentioned cases have a common aim – prevention the crystallite agglomeration, control the particle shape, size, size-distribution and crystal phase.

Moreover, some progresses have been made in understanding the role of the polymers on nucleation and crystal growth during ZnO synthesis. Nevertheless, there is still a further challenge to find simple and mild production routes, which will determine the realization of practical applications. Using functional polymer matrices as host molecules for nanoparticles will

* Corresponding author: vrinceanu.narcisa@ulbsibiu.ro, 0040721428641, 0040232202516

result in strong structural bounds between organic macromolecules and inorganic crystals.^{7,8} The explanation lays on the fact that the major part of organic materials is intercrystalline, and in a minor way intracrystalline. For these applications, the nanoparticles need to be dispersed homogeneously in the different matrices, and a number of new synthetic strategies have been developed in order to prevent particles agglomeration, and increase the stability of ZnO nanoparticles dispersions.^{9-13 a,b} For this purpose, there is a need of using a polymer matrix with a distinct advantage that is avoiding agglomeration of nanostructures.

Consequently, this research is aiming at a novel and facile approach to fabricate ZnO nanoparticles under the relatively simple and mild conditions, in which zinc nitrate is coated by MCT- β -CD. As a kind of cyclic oligosaccharide consisting of seven α -1,4 linked D-glucopyranose units, β -CD contains a toroidal hydrophobic cavity, which is capable of including a variety of inorganic and organic guest species.¹⁴⁻¹⁶ Presence of **β -cyclodextrin** (*i.e.* MCT) during ZnO synthesis can also ensure formation of different morphologies (micro-pellets, rods, plates, boxes, wires, tripods, tetrapods, nodular, irregular) of ZnO primary nanoparticles possessing different levels of zinc/oxygen concentrations and also different defect species dominance.¹⁷ Defects refer to intrinsic types including oxygen vacancies, zinc vacancies, zinc interstitials, oxygen interstitials and antisites species; these intrinsic defects tend to accumulate on the free surfaces (and internal interfaces) of ZnO particles, thereby determine the surface states that are known to be electrically and chemically active.

These **shape-dependent** impacts on ZnO potential applications (UV coatings, nanotextiles, photocatalysis and photodetection) reveal for the second time the motivation of this paper, the objective being the emphasizing the influence of functional polymers (**cyclodextrins**) properties – of forming chemical derivatives and inclusion compounds, namely grafting of a reactive CD derivative and the subsequent inclusion, in the grafted material, of guest compounds resulting new compounds. Since **cyclodextrins** (CDs) present nanocavities (0.57-0.97 nm in diameter) in which molecules of the same size order may be included, the second objective of the present study regarded the stability of ZnO nanoparticles dispersions, using such a polymer matrix, meaning a cyclic oligosaccharide, β -cyclodextrin (*i.e.* MCT), in the architectural structure of ZnO powders. MCT is a

biocompatible polymer and is known to form a wide range of inclusion complexes with several molecules.^{18,19}

In our present research, the parameters represented by the concentration of MCT is varied to study its impact on the ZnO morphology, dimension and intrinsic defects.

Taking into account the indices according to which zinc would have regenerative effects, stimulating osteogenesis,²⁰ using this new composite as support for bone formation is challenging (lamellar structure similar to calcite), as well as tissue engineering. During some experimental researches,²¹ the microscopic investigation revealed aspects of miofibroblasts proliferation in the geodes resulted from some silver doped nanoparticles polyurethane-urea subcutaneous implants degradation. The effect of silver nanoparticles to accelerate the curing of the wounds is mentioned, especially by means of fibroblasts differentiation into contractile miofibroblasts.²²

The same effect can be expected from the zinc nanoparticles, taking into account the effect of zinc supplementation on resistance of cultured human skin fibroblasts toward oxidant stress,²³ on one hand, and still at fibroblasts level, endogenous antioxidant enzymes induce myofibroblastic differentiation, on the other hand.²⁴ Having all these above mentioned, study of biocompatibility and *in vivo* effects of this composite is demanding.

1. Experimental sections

1.1. Synthesis of nano-ZnO

The zinc oxide (ZnO) nanoparticles were prepared by wet chemical method (sol-gel method)²⁵ using zinc nitrate and sodium hydroxide as precursors and soluble MCT as stabilizing agent.

Different amounts of soluble (MCT) (MCT₁ = 0.5%, MCT₂ = 1%, MCT₃ = 1.5%, MCT₄ = 2%) were dissolved in 500 mL of distilled water. Zinc nitrate was added in the above solution. Then the solution was kept under constant stirring using magnetic stirrer to completely dissolve the zinc nitrate. After complete dissolution of zinc nitrate, 0.2 mol of sodium hydroxide solution were added under constant stirring, drop by drop touching the walls of the vessel. The reaction was allowed to proceed for two hours after complete addition of sodium hydroxide. After the

completion of reaction, the solution was allowed to settle for overnight and the supernatant solution was then discarded carefully. The remaining solution was centrifuged at 10,000 rot/min for 10 min and the supernatant was discarded. Thus obtained nanoparticles were washed three times using distilled water. Washing was carried out to remove the byproducts and the excessive MCT that were bound with the nanoparticles. After washing, the nanoparticles were dried at 80°C for overnight. During drying, complete conversion of $\text{Zn}(\text{OH})_2$ into ZnO takes place.

1.2. Instrumentation for characterization of micro- and nano of ZnO

1.2.1. Morphological characterization of ZnO nanoparticles

The structure of ZnO – MCT powder has been analyzed through a co-assisted system: Scanning Electron Microscopy coupled with energy dispersive X-ray (EDX) investigation technique X Ray Diffraction and FTIR Spectroscopy.

X-ray diffractometry. X-ray Diffraction (XRD) data for structural characterization of the various prepared samples of ZnO were collected on a X-ray diffractometer (PW1710) using Cu-K α radiation ($k = 1.54 \text{ \AA}$) source (applied voltage 40 kV, current 40 mA). About 0.5 g of the dried particles were deposited as a randomly oriented powder onto a Plexiglass sample container, and the XRD patterns were recorded at angles between 20° and 80°, with a scan rate of 1.5°/min.

Scanning electron microscopy–energy-dispersive X-ray spectroscopy. Scanning electron microscope (SEM) images of the samples were obtained from a Quanta 200 3D Dual Beam type microscope, from FEI Holland, coupled at a EDS analysis system manufactured by EDAX –

AMETEK Holland equipped with a SDD type detector (silicon drift detector).

Taking into account the sample type, the analyses have been performed, using Low Vacuum working mode, allowing the probes testing in their initial state, without a previous metallization (as in High Vacuum working type). Both for the acquisition of secondary electrons images (SE – secondary electrons) and EDS type elemental chemical analyses, LFD (Large Field Detector) type detector has been used, running at a pressure of 60 Pa in working room, and a voltage of 30kV.

FTIR spectroscopy. FTIR was used to examine changes in the molecular structures of the samples. Analysis has been recorded on a FTIR JASCO 660 + spectrometer. The analysis of studied samples was performed at 2 cm^{-1} resolution in the transmission mode. Typically, 64 scans were signal averaged to reduce spectral noise.

RESULTS AND DISCUSSION

SEM images show a lamellar structure similar to those of biogenic ceramic materials, in particular calcites formed by the echinoderm intracrystalline and mollusk shell proteins (Fig. 1). It is noticeable a randomly distributed particles consisting of nanostructures in MCT matrix, which is equivalent with a good adhesion between the surface of ZnO nanoparticles and MCT matrix. SEM images from Fig. 1 presents ZnO crystals grown in the presence of the MCT which induced the formation of large well-developed rough planes. There is a remarkable analogy between the formation of crystalline faces already observed in biogenic calcites,²⁶ as function of the presence of carboxylate or sulfonate groups in the polymeric chain and the obtained pellets.



Fig. 1 – Similarities between studied lamellar structures of ZnO nanoparticles entrapped in MCT matrix and calcites from the literature.²⁶

The scale bars represent 20 μm . The new well-developed faces are almost parallel one to each other. The distribution of particles reflects lamellar structures. It is noticeable a randomly distributed protruding particles consisting of further nanostructures in polymer matrix, which is equivalent with a good adhesion between the surface of ZnO nanoparticles and MCT matrix. It is notable that large, well-defined faces are expressed at relatively high concentrations of MCT ($\text{MCT}_3 = 1.5\%$), compared with the untreated material (Fig. 2b).

Both Fig. 3a and 3b and Fig. 4a and 4b picture the morphology of the micro-pellets at different magnitudes: X300, X1200, X2400, X5000. It suggests that a two-length-scale hierarchical structure is formed on the surface. The nanoparticles are well dispersed in the MCT nanocavities, although some aggregated nanoparti-

cles are still visible. The particles size plays a primary role in determining their adhesion on an ipothetic fibrous matrix. This kind of structures is in accordance with water repellent properties exhibited by the lotus leaf.

The assistance of MCT during ZnO synthesis can ensure formation of micro-pellets with nanometric thickness. This texture is in accordance with the morphology of the single crystal elements, suggesting that MCT may also have influence in the shape of the crystal during growth. These micro-pellets can function as the building blocks for future nanoscale composites, as envisioned by Richard Feynman almost 5 decades ago.²⁷

The results of the **EDX elemental analysis** is shown in Fig. 5, indicating that ZnO nanoparticles contain approximately 80% ZnO, meaning that ZnO phase represented more than half of the sample mass.

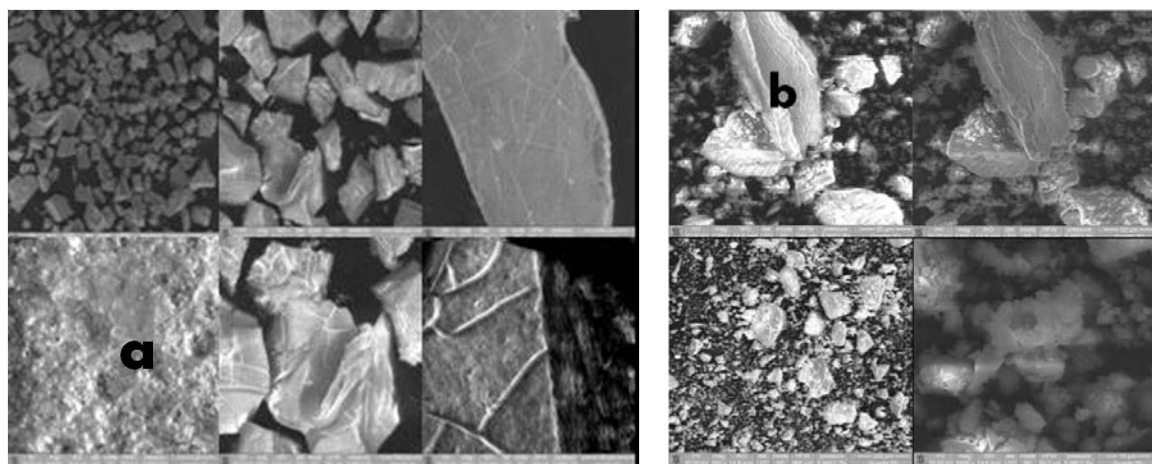


Fig. 2 – Scanning electron micrograph of zinc oxide embodied in: **a.** MCT_1 and **b.** MCT_2 matrices.

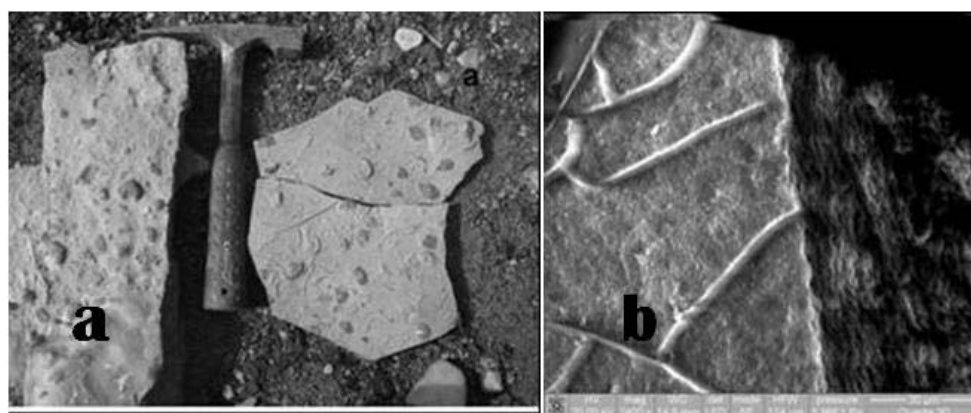


Fig. 3 – Similarities between calcites at macroscopic level (eye observation) – **a.**, and studied lamellar structures of ZnO nanoparticles entrapped in MCT matrix at microscale level – **b.**

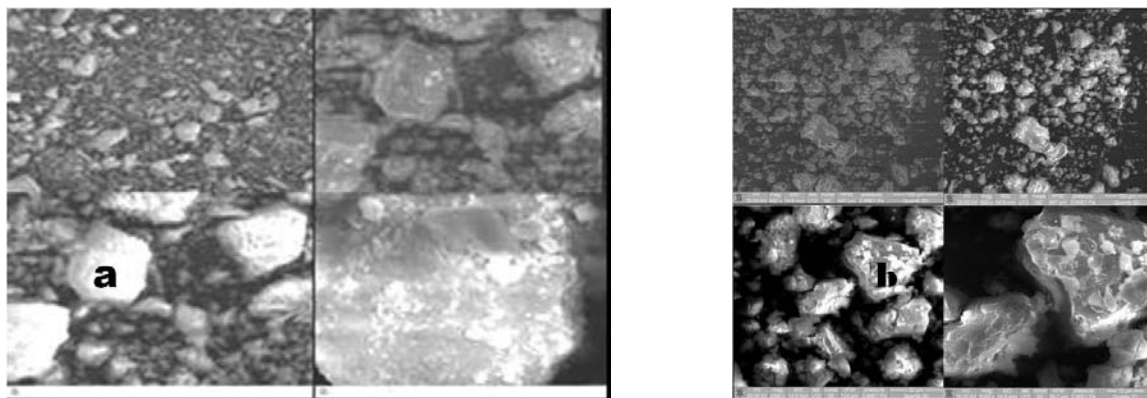


Fig. 4 – Scanning Electron Micrograph of Zinc Oxide embodied in **a** – MCT₃ and **b** – MCT₄ matrices.

Table 1

Surface composition for ZnO nanocrystals, from EDX measurements

Element	Wt%	At%
CK	14.23	43.43
OK	3.93	9.01
ALK	2.08	2.83
ZnK	79.76	44.74

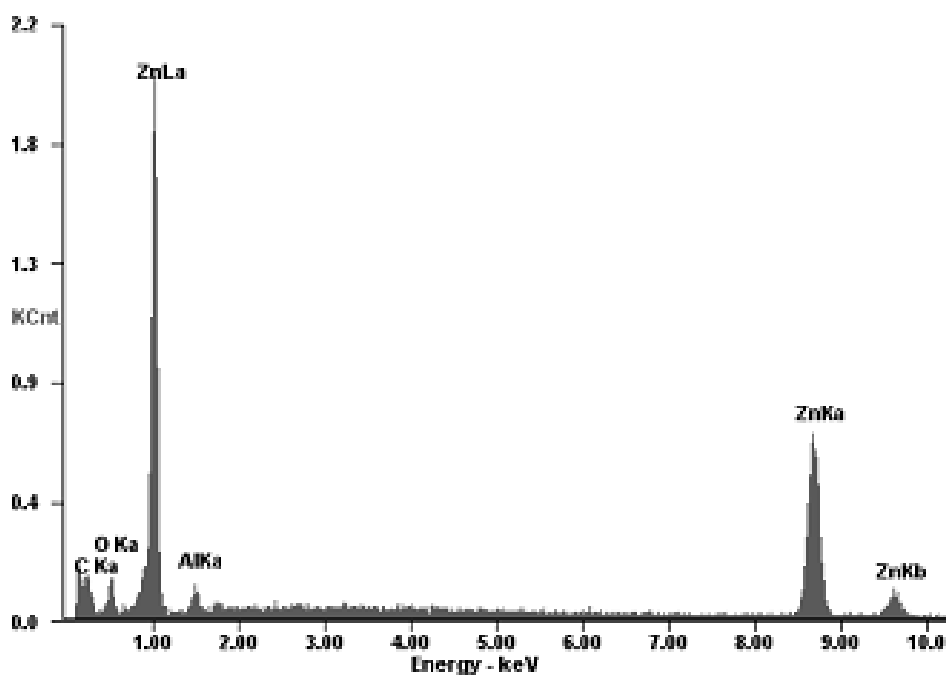


Fig. 5 – EDX analysis (Wt: weight percent, At: atomic percent).

Fig. 6 shows the XRD patterns of ZnO nanocrystals entrapped into MCT₁, MCT₂, MCT₃ and MCT₄ polymer matrices. The peaks assigned to diffractions from various planes correspond to hexagonal close packed structure of zinc oxide. The broadening of peaks was observed mainly due to the nano-size effect. The broad reflection at 25°

is due to the low crystallinity of the soluble MCT. Presence of MCT in the completely washed nano-ZnO indicates their strong binding nature. Peaks at scattering angles (2θ) of 26.5737, 33.72, 38.03, 51.87, 64.71 and 71.32 indicate the crystallinity of the synthesized solid.

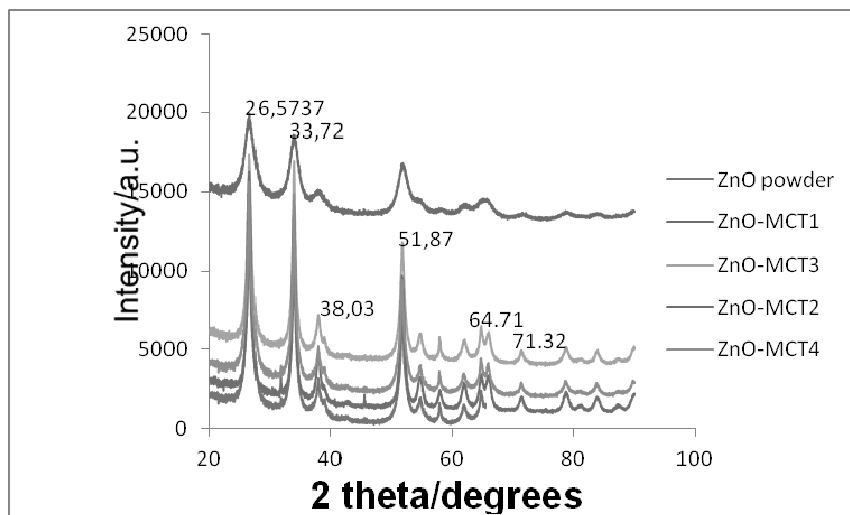


Fig. 6 – XRD pattern of nano ZnO entrapped in different concentrations of MCT; a – ZnO-MCT₁; b – ZnO-MCT₂; c – ZnO-MCT₃; d – ZnO-MCT₄.

The XRD pattern is identical to the hexagonal phase with Wurtzite structure (hexagonal phase) unit cell Parameters $a = b = 3.248 \text{ \AA}$ and $c = 5.2 \text{ \AA}$.

Rather broad diffraction maxima indicate very small size of the crystallites similar to the size of subunits observed by the SEM (Figs. 1-4). Meanwhile, no diffraction peaks from other species could be detected, which indicates that all the precursors have been completely decomposed during the sol-gel process. It is noteworthy that encaving/entrapment process of ZnO particles into cyclodextrin matrices induced the augmentation of compound crystallinity with the respect to multiplying of peaks (64.71 and 71.32) for ZnO-MCT₂, ZnO-MCT₃ and ZnO-MCT₄ indexed samples. In our case, the increasing of MCT concentration did not mean an improvement of crystallinity, since the XRD pattern attributed to ZnO-MCT₃ and ZnO-MCT₄ compounds seem to have a lot of similarities.

The use of FT-IR technique allows the detection of complex formations in solid phase and points out the implication of the different functional groups of guest and host molecules in the inclusion process by analyzing the significant changes in the shape and position of the absorbance bands of zinc oxide powder, monochlorotriazinyl- β -cyclodextrin, physical mixture and inclusion complexes.

Fig. 7 reveals some dominant features in the infrared spectrum of the ensemble of ZnO powders: Zn-O absorption band near 430 cm^{-1} . Theoretically, MCT exhibited significant FT-IR peak at wave number of 955, 1093, 1241, 1443, 2321 cm^{-1} . The monochlorotriazinyl- β -cyclodextrin in the synthesized powder is shown by the

1400 cm^{-1} vibration band corresponding to the -C=N- group from the triazinic nucleus. The spectrum of ZnO embodied in MCT- β -CD, compared with that belonging to MCT- β -CD have the same bands, characteristic for triazinic nucleus $\nu(\text{C}=\text{N})$ meaning: at 1608 , 1570 and 1471 cm^{-1} for MCT- β -CD. It is noteworthy that the band at 1570 cm^{-1} characteristic for triazinic nucleus $\nu(\text{C}=\text{N})$, decreased in intensity from the complex ZnO-MCT₄ – having the highest concentration of MCT, to ZnO-MCT₁ (the lowest concentration of MCT). This reveals that ZnO nanoparticles have been indeed entrapped within the reactive matrix monochlorotriazinyl- β -cyclodextrin. The small shifts of the bands characteristic to triazinic nucleus is due to the substituent modification (from -Cl in -O-R), following the reaction between and zinc nitrate. Here is a broad band with very low intensity at 3493 cm^{-1} corresponding to the vibration mode of water OH group indicating the presence of small amount of water adsorbed on the ZnO nanocrystal surface. The band at 1628 cm^{-1} is due to the OH bending of water. Moreover, intense peak at 1710 cm^{-1} (carbonyl group) is noticeable.

The band at 500 cm^{-1} is attributed to the Zn-O stretching band which is consistent with that reported.^{32,33} This mentioned band intensity is also the highest in case of the highest concentration of MCT (ZnO-MCT₄ compound) and become very low as intensity in case of ZnO – MCT₁ complex. Consequently, it can be claimed that FT-IR spectra completes/filled the results provided by the previous analysis, highlighting the primary/important incontestable role of MCT, in encaving the ZnO particles within polymer matrix.

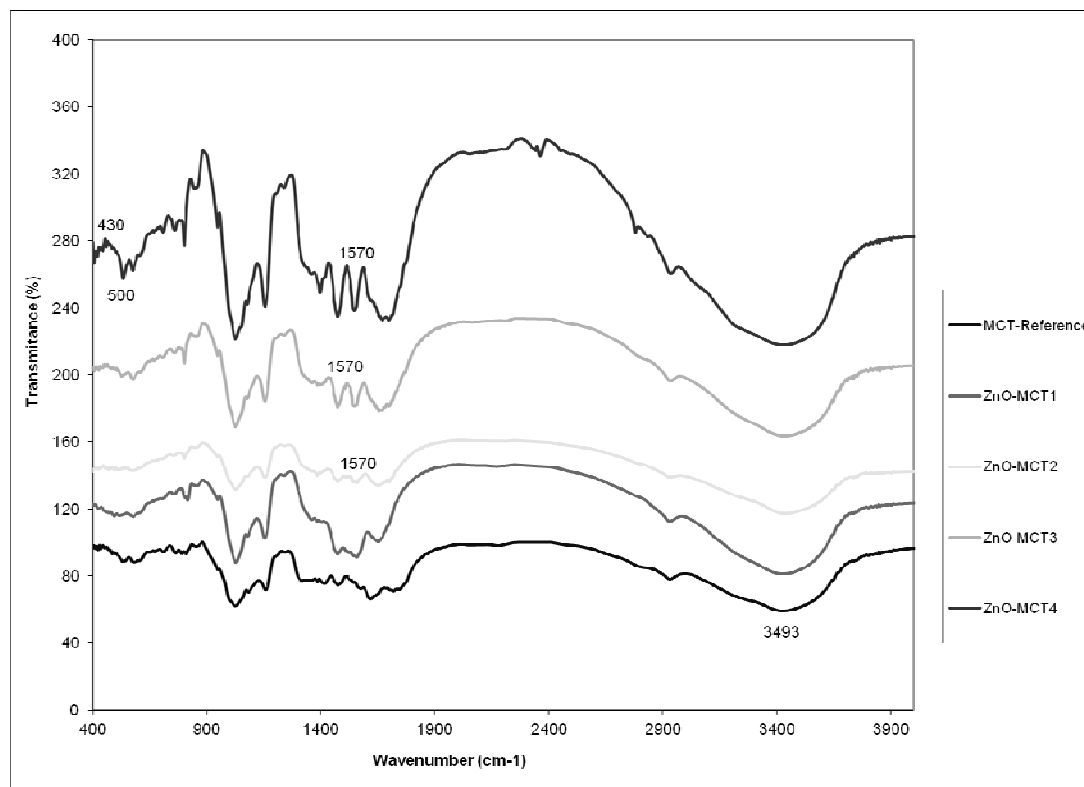


Fig. 7 – FT-IR Spectra of ZnO powders (ZnO-MCT1; ZnO-MCT2, ZnO-MCT3; ZnO-MCT4), compared with MCT spectrum.

Because, this study is a preliminary one, our perspective study will be oriented in achieving a textile nanoacomposite with an architecture allowing blocking of different guest compounds, with different properties like: water repellence, antimicrobial activity, photoprotection etc.

Consequently, the particles size plays a primary role in determining their adhesion to the fibers: it is reasonable to expect that the largest particle agglomerates will be easily removed from the fiber surface, while the smaller particles will penetrate deeper and adhere strongly into the fabric matrix.

CONCLUSIONS

Based on the analysis of the results of the experimental study the following conclusions can be drawn.

This research provides a novel and simple method of growing of ZnO–monochlorotriazinyl- β -cyclodextrin nanocomposites via a facile method. Due to the assistance of monochlorotriazinyl- β -cyclodextrin, using nitrate as crystal growth modifier, the approached synthesis showed a lamellar ZnO nanostructure. In other words, the study revealed a surprisingly structural similitude between ZnO nanoparticles and natural biocomposites.

The microstructures were studied by a co-assisted system: X-ray diffraction method, scanning electron microscopy, FT-IR spectroscopy techniques. On the basis of the investigation on the growth process monochlorotriazinyl- β -cyclodextrin–ZnO interaction was vital to the formation of complex structure, forming the high-quality lamellar nanostructures. It has been observed that the morphology, dimension, and size distribution of the product ZnO are strongly affected by the presence of monochlorotriazinyl- β -cyclodextrin.

The above SEM figures suggested that a two-length-scale hierarchical structure is formed on the surface. The nanoparticles are well dispersed in the MCT nanocavities, although some aggregated nanoparticles are still visible. The particles size plays a primary role in determining their adhesion on an ipothetic fibrous matrix. This kind of structures is in accordance with water repellent properties exhibited by the lotus leaf.

In order to achieve selective growth of a desired morphology, understanding on the nanostructure morphology can be considered assistance in monitoring fabrication processes. In return, unique quantum confinement effects can be maximized from the desired crystallographic orientations that in the future will lead to a prototype novel nanodevices of important commercial value.

Taking into account the composite lamellar-porous structure, the results of the present work could be leveraged in the area of tissular engineering or for the manufacturing of some wound dressing. There is the possibility that zinc could stimulate the osteogenesis and, by similitude with silver, could accelerate the wound cure through fibroblasts differentiation into microfibroblasts.

As perspective, textural information achieved in this research – the porous-lamellar structure – will be used *in vitro* studies, concerning the utilizing of the composite, as bandage or in tissue engineering.

Acknowledgements: This work was partially supported by a grant of the Romanian National Authority for Scientific Research, CNCS – UEFISCDI, project number PN-II-RU-TE-2012-3-0202. Moreover, the authors are grateful to the financial support provided both Research POSDRU/89/1.5/S/49944 Project, belonging to “A.I. Cuza” University of Iași.

REFERENCES

1. A. Taubert, D. Palms, O.O. Weiss, M-T Piccini M-T, D.N. Batchelder, *Chem. Mater.*, **2002**, *14*, 2594.
2. M.H. Huang, Y.Y. Wu, H.N. Feick, N. Tran, E. Weber, P.D. Yang, *Adv. Mater.*, **2001**, *13*, 113.
3. K. Vanheusden, K. C.H. Seager, W.L. Warren, D.R. Tallant, J.A. Voigt, *Appl. Phys. Lett.*, **1996**, *68*, 4034.
4. J. Zhang, L.D. Sun, H.Y. Pan, C.S. Liao, C.H. Yan, *New J. Chem.*, **2002**, *26*, 33.
5. S. Fujihara, C. Sasaki, T. Kimura, *Appl. Surf. Sci.*, **2001**, *180*, 34.
6. T.J. Gardner, G.J. Messing, *Thermochim. Acta*, **1984**, *78*, 7.
7. B. Chen, X. Peng, J. Wang, S. Sun, *Comp. Mat. Sci.*, **2008**, *4*, 201.
8. B.L. Smith, T.E. Schaffer, M. Viani, J.B. Thompson, N.A. Frederick, J. Kind, A. Belcher, G.D. Stucky, D.E. Morse, P.K. Hansman, *Nature*, **1999**, *399*, 761.
9. L. Guo, S. Yang, C. Yang, P. Yu, J. Wang, W. Ge, G.K.L. Wong, *Chem. Mater.*, **2000**, *12*, 2268.
10. Y.J. Kwon, K.H. Kim, C.S. Lim, K.B. Shim, *J. Ceramic Process Res.* **2002**, *3*, 146.
11. R.H. Wang, J.H. Xin, X.M. Tao XM, *Inorg. Chem.*, **2005**, *44*, 3926-3930.
12. S. Liufu, H. Xiao, M. Li, *Powder Technol.*, **2004**, *145*, 20-24.
- 13a. E. Tang, G. Cheng, X. Ma, *Powder Technol.*, **2006a**, *161*, 209-214.
- 13b. E. Tang, G. Cheng G, X. Ma, X. Pang, Q. Zhao, *Appl. Surf. Sci.*, **2006**, *252*, 5227-5232.
14. M.L. Bender, M. Komiyama, “Cyclodextrin Chemistry”, Springer, Berlin 1978.
15. J. Szejtli, “Cyclodextrins and their Inclusion Complexes”, Akadmiai Kiado, Budapest 1982.
16. G. Wenz, *Angew. Chem.*, **1994**, *33*, 803.
17. B.M., Shahrom, “Synthesis and characterization of zinc oxide nanostructures”, Universiti Sains Malaysia, 2008.
18. R.C. Bergamasco, G.M. Zanin, F.F. De Morales, *J. Incl Phenom Macrocyclic Chem.*, **2007**, *57*, 157.
19. T. Furuta, Y. Kusuya, T.L. Neoh, L. Rehmann, S.H. Beak SH, H. Yoshii, *J. Incl Phenom. Macrocyclic Chem.*, **2006**, *56*, 107.
20. A. Ito, *Curr. Appl. Phys.*, **2005**, *5*, 402-406.
21. B.A. Hagi, L.C. Burtan, M.S. Mihailovici, V. Tura, C. Ciobanu, D. Ferariu, *Lucrări Științifice, seria Medicina Veterinară*, **2006**, *40*, 97-101.
22. P.S. Melo, P.D. Marcato, S.C. Huber, I.R. Ferreira, N. Durán, S. Torsoni, A.B. Seabra, O.L. Alves, *J. Phys.: Conference Series* **2011**, *304*, 012027.
23. M.J. Richard, P. Guiraud, M.T. Leccia, J.C. Beani, A. Favier, *Biol. Trace Elem. Res.*, **1993**, *37*, 187-199.
24. E. Artaud-Macari, D. Goven, S. Brayer, A. Hamimi, V. Besnard, J. Marchal-Somme, Z.E. Ali, B. Crestani, S. Kerdine-Römer, A. Boutten, M. Bonay, *Antioxid Redox Sign.*, **2013**, *18*, 66-79.
25. D. Tanasa, N. Vranceanu, A. Nistor, C.M. Hristodor, E. Popovici, I.C. Bistriceanu, F. Brînza, D.-L. Chicet, D. Coman, A. Pui, A. M. Grigoriu and G. Broasca, *Text. Res J.*, **2012**, *82*, 832-844.
26. http://www.google.ro/search?q=biogenic+calcites&hl=ro&biw=1366&bih=624&prmd=ivnsb&source=lnms&tbn=isch&ei=fWoHTpqFKNGaOv6S7bgN&sa=X&oi=mode_link&ct=mode&cd=2&ved=0CA0Q_AUoAQ
27. P.W. Christopher, P. Weiss, H.J. Bruce, *J. Sedimentary Research*, **1988**, *58*, 479-488.